Available online at http://www.ijasrd.org/in

International Journal of Advanced Scientific Research & Development

Vol. 03, Iss. 01, Ver. II, Jan – Mar' 2016, pp. 109 – 125

e-ISSN: 2395-6089
p-ISSN: 2394-8906

SYNTHESIS AND CHARACTERIZATION OF ZNO NANOPARTICLES FOR CHEMIRESISTIVE AMMONIA VAPOR SENSOR

S. Fairose

Ph.D., Research Scholar, PG & Research Department of Physics, Urumu Dhanalakshmi College, Trichy – 620 019, Tamilnadu, India.

Dr. Suhashini Ernest*

* Corresponding Author, Associate Professor & Head (Retd.), PG & Research Department of Physics, Urumu Dhanalakshmi College, Trichy – 620 019, Tamilnadu, India.

ARTICLE INFO

Article History:

Received: 28 Feb 2016;
Received in revised form:
05 Mar 2016;
Accepted: 05 Mar 2016;
Published online: 31 Mar 2016.

Key words:

N-ZnO,
Ammonia Vapour,
Sensor,
Sensitivity,
Spray Pyrolysis,
Topographical Properties,
Thin Film

ABSTRACT

Zinc oxide (ZnO) thin films with various concentrations were deposited onto glass substrates by using the spray pyrolysis technique at 230oC substrate temperature. Structural, optical and morphological studies of the samples were characterized using XRD, UV-Vis-NIR spectroscopy, atomic force microscopy (AFM) and field emission scanning electron microscopy (FESEM) respectively. The X-ray diffraction analysis reveals the hexagonal wurtzite structure of the ZnO thin films. An increase in crystal size and roughness with increase in concentration of the precursor solution is observed from the AFM studies. The morphological studies reveal that all samples are polycrystalline in nature. The optical study implies that the absorbance increased with increasing molar concentration. The ZnO films showed high transparency nearly 80% in the visible and NIR regions at lower concentrations and the band gap values are found to be in the range of 3.25 eV to 3.32 eV. A high sensitivity for NH3 was obtained for the ZnO film at 0.1 M. The sensing response of 0.1M ZnO sample towards NH3 vapor has been investigated at different vapor concentrations at 300oC temperature.

INTRODUCTION

ZnO has a wide band gap (~3.37eV) with large binding energy (60meV) that enables the use of Zinc Oxide thin films for organic light emitting diodes and efficient UV lasers. It

How to cite this article: Fairose, S., & Ernest, S., (2016). "Synthesis and Characterization of ZnO Nanoparticles for Chemiresistive Ammonia Vapor Sensor". *International Journal of Advanced Scientific Research & Development (IJASRD), 03* (01/II), pp. 109 – 125.

is a semiconductor of the II-IV family with hexagonal wurtzite structure. It has good electrical, optical, and piezoelectric properties. Also it has high mobility of conduction electrons, excellent stability and is of low cost[1]. It has numerous applications such as, photo catalysis[2], solid state optoelectronic devices[3][4][5], dye-Sensitized solar cells[6][7], gas sensors[8][9] and heterojunctions[10]. Its interesting wetting properties are also important for many industrial processes, such as cleaning, drying, paint coating, adhesion, heat transfer, and pesticide applications. Various physical and chemical techniques are used to prepare thin films, such as RF magnetron sputtering[11], chemical vapour deposition[12], thermal evaporation[13], spray pyrolysis technique (SPT)[14][15] and successive ionic layer adsorption and reaction (SILAR)[16].

Among these methods, SPT is an important technique that is very simple, low cost, and can be easily handled. Also, it can be used effectively for large area deposition. There are several reports available in the literatures that are related to the ZnO thin films by SPT and its different kinds of applications. N. L. Tarwal et al.,[17] reported the multifunctionality of ZnO thin films synthesized by spray pyrolysis and discussed ethanol and propanol sensing performance. P. Mitra et al.,[18] reported the electrical properties of chemically deposited ZnO films and their gas sensing characteristics to hydrogen and liquefied petroleum gas and the sensitivity to target gas has been studied in terms of degree of lowering of sensor resistance. R. Ferro et al.,[19] suggested the work of correlation between thickness, morphology and NO_2 response of ZnO thin films. T.V Vimalkumar et al.,[20] carried out structural, electrical, and optical studies and analysed the relation between the concentration of precursor solution and the optoelectronic properties of the ZnO films. F.Paraguay et al.,[21] investigated the sensing properties of spray pyrolytic ZnO-doped thin films, to ethanol vapour. Jiaqiang Xu et al.,[22] explained the alcohol sensing mechanism of ZnO and Ru-doped ZnO, on the basis of analysing catalytic oxidation products of C_2H_5OH and the relation between the conversion ratio and gas response of C_2H_5OH. P.S. Shrwale et al.,[23] reported the structural, morphological, electrical properties of ZnO thin films and also reported the H_2S gas sensing properties at different operating temperatures with lower concentration.

In this present work, ZnO thin films were deposited on the glass substrate using the spray pyrolysis technique. Structural, morphological and optical properties of ZnO films were studied as a function of solution concentration. Also, the vapor sensing performance of the samples was studied at 0.1M concentration.

EXPERIMENTAL DETAILS

ZnO thin films were deposited onto the glass substrates using spray pyrolysis technique. De-ionized water was used as solvent for preparing the precursor solution. In the present study, the precursor solutions of four different concentrations of 0.05 M, 0.1 M, 0.15 M and 0.2 M were prepared by dissolving Zinc acetate[$Zn(CH_3COO)_2.2H_2O$] in deionised water. The distance between the substrate and the spray nozzle was kept constant at 30cm and at an angle of 45^0. The spray rate and temperature were held constant at 2ml/min and $230^oC \pm 2^oC$ respectively. Illustration of the formation mechanism of Spray deposited ZnO thin film reaction is given in Fig. 1.

These films were further used to investigate the morphological, optical, structural, and gas sensing properties. Crystallinity of the films was analysed using Rigaku (D.mac.c) X-ray diffractometer (CuKα line; λ=1.5405Å). Surface morphology of the sample was studied using scanning electron microscopy (JEOLJSM-840). Optical absorbance and transmittance of the samples at normal incidence were analysed using UV-Vis-NIR spectrometer (Jasco-V-570). Sensor resistance was obtained using Lab VIEW-controlled NI USB 6212 data acquisition board interfaced to a computer. Electrical leads were made by using silver epoxy and thin copper wire. Vapor response of the film was studied by the chemiresistor method and the response was calculated using the relation R_{air}/R_{gas}, where R_{air} and R_{gas} denote the resistance values in air and NH_3 atmosphere respectively.

RESULTS AND DISCUSSION

3.1 Structural Characteristics

X-ray diffraction patterns of ZnO thin films with various precursor solution concentrations are given in Fig. 2. The presence of all peaks ware indexed to the standard XRD spectrum of the ZnO structure in accordance with JCPDS card No. 00-036-1451. All films exhibited a high intensity (main peak) attributed to the (101) plane. Other peaks represent low intensity (100) and (002) diffraction peaksThe intensity of the (101) plane at 36.28°is significantly higher than other peaks[24-26].

Results from the XRD studies show that the samples have polycrystalline nature, irrespective of the variation in concentration. The texture co-efficient (TC) was calculated for the different planes using the following expression.

$$TC(hkl) = \frac{I(hkl)/I_r(hkl)}{[(1/n)\sum I(hkl/I_r(hkl))]} \quad \text{----------1}$$

where I(hkl) indicates the X-ray diffraction intensity obtained from the film, I_r is the intensity of reference diffraction pattern and 'n' is the number of diffraction pattern (JCPDS data card (36-1451)). It is clear from the definition that the variation of the texture co-efficient implies the film growth in preferred orientations. Texture co-efficient calculated for different orientations namely (101), (100), (002) and (110) are shown in Table 1. These results indicate that the ZnO thin film does not grow well at a lower concentration due to an insufficient amount of the Zn^{2+} species, resulting in slower ZnO growth than the films grown at higher concentrations[27].

Crystallite size was calculated for (101) at the maximum diffraction peak value using Debye Scherrer formula, the crystallinity increased with increase in solution concentration[28]

$$D = \frac{k\lambda}{\beta\cos\theta} \quad \text{----------2}$$

where D is the diameter of the crystallite, λ is the wave length of the CuKα line (λ=1.5404Å), β is the full width at half maximum in radians and θ is the Bragg angle. The dislocation density (δ), defined as the length of dislocation lines per unit volume of the crystal, is calculated using the following formula(3) by Saleem et al.,[29] and specific surface area of the ZnO crystallite was calculated using equation (4) by Jonnala Rakesh Reddy et al.,[30]

$$\delta \equiv 1/D^2 \text{----------3} \qquad A = \frac{6}{D \times \rho} \text{----------4}$$

where 'A' is the specific surface area, 'D' is the crystallite size and 'ρ' is the density of ZnO (5.606 g m^{-3}). Surface area of 0.1M is higher than other precursor solution concentration. This parameter calculated from the XRD data is given in Table 2

The lattice constants 'a' and 'c' were calculated by using the following equations 5 and 6 by Nanda Shakti et al.,[31]

$$a = \sqrt{\frac{1}{3}}\frac{\lambda}{\sin\theta} \text{----------5} \qquad c = \frac{\lambda}{\sin\theta} \text{----------6}$$

The observed 'c' and 'a' values given in Table 3 are in agreement with the standard values taken from JCPDS data card (36-1451). In thin films, strains originate mainly because of lattice mismatch between the film and the substrate and the differences in co-efficient of thermal expansion of the film and the substrate. Strain value was calculated using the following expression.

$$\varepsilon = \frac{\beta \cos\theta}{4} \text{----------7}$$

Strain(ε)% of the thin films is calculated from the c-axis lattice parameter using the following formula by Benramache et al.,[32]

$$\varepsilon\% = \frac{C - C_0}{C_0} \times 100 \text{----------8}$$

Where C is the lattice parameter of ZnO films calculate from XRD data and C_0=5.205Å is the unstrained lattice parameter of ZnO.

Strain could be positive (tensile) or negative (compressive) according to the above equations (7) and (8) shown in Table (2). These calculated values of strain along with the peak position for (101) are tabulated in Table 2. According to the above formula, the positive values of ε represent tensile strain while a negative value represents compressive strain. As the ZnO content increases, the concentration of the film also increases, indicating that as the film grows thicker, and the film is relaxed by reducing the strain. The film that has concentration of 0.1M shows the minimum strain. The evaluated structural parameters of ZnO thin films using its (101) orientation are presented in Table 2, showing that the strain in the spray pyrolysis method derived ZnO films is tensile and the optimum concentration of film approximately 0.1M for the best structural quality. According to Ghosh et al.,[33] the tensile strain might be due to a thermal mismatch between the ZnO film and glass substrate. From the dislocation density data, one can clearly observe that the crystallite of the films is good because of their small dislocation density (δ) values, which represent the amount of defects in the film. The larger D and smaller dislocation density (δ) values show better crystallization of the films.

3.2 Surface Morphological Studies

3.2.1 FESEM

The thickness of the samples, studied using profilometer, is found to increase with increasing concentration of the precursor solutions (98nm, 185nm, 280nm and 366nm for 0.05M, 0.1M, 0.15M and 0.2M respectively). The FESEM morphologies of the ZnO thin films coated at different concentrations are shown in Fig.3. The surface morphology of the film at 0.1M indicates appreciable formation of nanoparticles of ZnO. The grain size (D) of ZnO has increased from 7.8 to 15.7 nm as a function of concentration. The coated films become thicker as the concentration increases. More Zinc particles are present in thicker films increasing the electrostatic interaction between the particles facilitating the congregation of particles to form a grain[34]. Thus the grain size increases as concentration is increased. The presence of the nanoparticles with increasing porous structure is more clearly observed in the film morphology for thicker films.

.

3.2.2 Atomic Force Microscopy

AFM measurements of surface topography of the film were carried out using a Shimadzu atomic force microscope in contact mode. A commercial standard pyramidal Si3N4 tip was used. An AFM image was acquired in ambient air and digitized to 256*256 pixels. AFM image of ZnO thin films with 0.1M and 0.2M as shown in Fig. 4 and 5 The RMS(root-mean-square) roughness values of sample (0.1M) and (0.2 M) are 13.5nm and 45nm respectively. As can be seen, the micrographs reveal that the films are closely packed and granular in nature. 0.2M of ZnO film has a high dense roughness value compared to the 0.1M sample. The roughness value increases with increase in solution concentration.

3.3 Optical Properties

Fig. 6 shows the absorbance spectra of ZnO thin films deposited at different molar concentrations in the wavelength range of 300-1200 nm. It is observed from the figure, the absorption edges are below 380nm for all concentrations. Which can be attributed to the intrinsic band gap of the ZnO due to electron transitions from the valence band to the conduction band.

Optical transmission spectra of ZnO films in the range of 300-1200 nm wavelength range are presented in Fig.7. The transmission decreased sharply near the ultraviolet region at approximately 380 nm for all the, films corresponding to the intrinsic band gap energy of ZnO. Higher transmittance (nearly 80%) is achieved at a lower concentration (0.05M). At higher solution concentrations (>0.05M), the ZnO thin films exhibited a decrease in the optical transmittance due to the formation of larger particles, film thickness and void around the grains as presented in FESEM results. The decrease in transmittance may also be due to increase of the optical scattering caused by the grain boundaries. The optical band gap energy (Eg) values of the films were calculated by applying the Tauc model, given in the following relations[35]

$\alpha = (2.303A)/t$ ---------- (9)

$\alpha h\nu = B\sqrt{h\nu - E_g}$ ----------(10)

where α is the absorption coefficient, hv is the photon energy, Eg is the optical band gap and B is constant. The optical band gap values, Eg, of the ZnO films were obtained from

the absorption coefficient measurements by plotting $(\alpha hv)^2$ versus hv. From the Tauc plot, the optical band gap energy of the ZnO thin films was found to range between 3.253 and 3.37 eV given in Fig 8 and Table 2, which is in close agreement with the values reported by other researchers for polycrystalline ZnO thin films[36].

3.4. Sensing Studies

3.4.1. Sensing Response to Different Reducing Vapors

Most of the metal oxides exhibit response changes when exposed to different vapors[37]. The sensing response of the spray deposited ZnO thin film towards other reducing vapors such as humid air (relative humidity = 54%), formaldehyde, acetone, and methanol in dry air atmosphere was studied without changing other experimental conditions. Fig. 9 picturizes the sensing response of ZnO film for individual vapors. The results reveal that ZnO film has a good sensing response towards ammonia than other reducing vapors at 300°C temperature. The selectivity of the film towards a particular vapor can be expressed as follows:

$$\text{Selectivity}=S_A/S_B \quad \text{----------(11)}$$

where S_A and S_B are the sensing responses of the film towards ammonia (target) vapor and interfering vapor respectively. The obtained result shown in Fig.10 indicates that ZnO thin film is highly selective towards ammonia vapor. The catalytic effect of nanostructured ZnO thin film increases the number of chemisorbed oxygen ions over the film surface and promotes the reaction with ammonia vapor. Moreover, the crystalline film being highly oriented could be a potential reason for increased selectivity[37] (P.S.Shewale *et al* 2012) towards ammonia vapor at 300° C temperature. The larger value of selectivity for a specific gas denotes that the sensor has a better competency to differentiate the target vapor (ammonia) from the other vapors. Therefore, a good sensing performance of 0.1M ZnO film sensor to NH_3 vapor was observed.

3.4.2 Temperature Effects of ZnO thin film

Temperature effects indicate that the film is sensitive enough for monitoring low concentrations (10 ppm) of ammonia vapor. The sensor response of ammonia vapor at different operating temperatures was evaluated Fig. 11. It shows the sensitivity as a function of operating temperature for ZnO film. This figure reveals that the maximum sensitivity (833%) is obtained at 300°C. It is well known that the sensitivity of the metal-oxide semiconductor sensor is mainly determined by the interactions between the target vapor and the surface of the sensor. So, it is obvious that for a greater surface area of the materials, the interaction between the adsorbed vapors and sensor surface are stronger, i.e. gas sensitivity is higher[38].

The sensor response rapidly increases with temperature, showing a maximum value at about 300° C and further increase in temperature causes a drastic decrease in the response. This volcano-like behavior can be interpreted and the resistance of the thin film material should decrease upon contact with ammonia vapor, because of release of free electrons in the bulk. However, in the range of low-mild operating temperatures, the sensor response is low because NH_3 molecules are not activated enough to react with the oxygen species adsorbed onto the semiconductor sensing layer. Increasing the temperature up to 300° C, the above described process occurs more easily, contributing to the high response

registered at this temperature (300° C). Raising the temperature above this value is deleterious for the ammonia sensing properties, because NH_3 and adsorbed oxygen desorption processes become predominant, making less available these reactive species on the ZnO surface.

3.4.3. Sensing Mechanism of ZnO Film for Ammonia (NH_3) Vapor

Commonly, the gas sensing mechanism of the semiconducting metal oxide gas sensors is based on variation in the electrical resistance or conductance due to vapor adsorption and desorption on the sensor surface. For example, when a ZnO-based sensor is exposed to air, oxygen from the ambient air adsorbs on the ZnO surface to form mainly O_2-, $2O-$ or $2O_2-$ depending on the operating temperature by capturing electrons from the ZnO conduction band [39], according to the following surface reactions

$O_2 + e- \rightarrow O_2 -$; $O_2 + 2e- \rightarrow 2O-$; $O2 + 4e- \rightarrow 2O_2-$.---------- (12)

The chemisorbed oxygen species are also known to depend on the grain size and film porosity[40]. Considering that ZnO is n-type, the number of majority carriers (electrons) decreases because of these surface reactions and thus ZnO thin films are supposed to exhibit quite a high resistance in air. When sensors are exposed to a reducing gas such as NH_3 vapor, the vapor reacts with the adsorbed oxygen species, producing NH_3 molecules and releasing electrons back into the conduction band:

$2NH_3 + 3O^-(ads)$ ----------$N_2 + 3H_20 + 3e^-$ ---------- (13)

These reactions cause an increase in conductivity and as observed, the resistance of ZnO-based vapor sensor is decreased. Schematic diagram of the possible ammonia sensing process of ZnO sensor is given in Fig 12.

The resistance response curve of ZnO thin film deposited at 0.1M precursor solution at 300°C for various gas concentrations of ammonia ranging from 10ppm to 50ppm is presented in Fig. 13. At each concentration, the initial resistance of the sensor in the dry air is high and steady, whereas its resistance decreases abruptly when it is exposed to NH_3 gas, exhibiting n-type semiconducting behaviour as expected. The lower initial resistance at lower concentration is also ascribed to the semiconducting property of the ZnO film. It is clear that the response characteristics of the sensor depend on the gas concentration.

3.4.4 Response and Recovery Time

Fig. 13 displays the transient response of the ZnO film for different ammonia concentrations from 10 to 50 ppm. An instantaneous change in film resistance was observed when exposed to ammonia vapor. This indicates the rapid response of ZnO film towards ammonia vapor and this is due to Nano crystallite present over the surface of the film, which enhances the reaction rate. Fig.14 indicates the response time (90sec) and recovery time (37sec) for ZnO thin film sensor to NH_3 at 10 ppm concentration maintained at a temperature of 300°C. At lower ammonia concentration, the interacting rate of the molecules over the surface of the film is low, thereby longer response was observed. On the contrary, at lower concentration, more number of adsorbed molecules could be desorbed at 300°C temperature, causing decrease in recovery time given in Table 4.

3.4.5 Rate of Response (Sensitivity)

It is seen that the resistance of ZnO thin film decreases in response to increasing concentration of ammonia (NH_3) gas. The resistance response of sensor structure was transformed into a sensitivity value using commonly used formula for the reducing gases given in eqn 14.

$$S = \frac{Ro - Rg}{Rg} \times 100\% \quad \text{----------(14)}$$

The sensitivity of zinc oxide film grown by the spray pyrolysis technique and their sensing properties are shown in Fig.15. The sensitivity of the film at high concentration (50 ppm) of ammonia was found to be appreciable and better, compared to the response at lower concentrations. Moreover, the porous structure of nano particles of the ZnO film is favorable for surface interaction between adsorbed oxygen ion (O_2^-) and ammonia vapor molecule.

CONCLUSION

(i) The ZnO thin films prepared by the spray pyrolysis technique using Zn $(CH3COO)_2 \cdot 2H_2O$ as the precursor are found to have hexagonal wurtzite structure with crystallite sizes of 7.8 nm to 15.7 nm and lattice strain of 0.0027 to 0.00415. The lattice parameters a (2.866 A˚ to 3.013A˚) and c (4.964 A˚ to 5.220 A˚) calculated from the diffraction data in the present investigation are found to be in close agreement with those reported in JCPDS card 36.1415 (a = 3.24A˚, c = 5.20A˚).

(ii) The transmittance of the samples is in the ranges from 400nm to 1200nm and optical absorbance studies are in congruence leading to the formation of good quality film.

(iii) ZnO films were investigated in the monitoring of NH_3 showing the maximum response at 300°C. The higher response was obtained for the NH_3 sensor based on ZnO thin film exhibiting randomly oriented morphology.

(iv) AFM images reveal that the ZnO films at 0.2M concentration exhibit a much rougher surface topography with a root mean square (RMS) roughness of 45 nm compared with that of the 0.1M film having a low RMS roughness of 13.5nm.

(v) In summary, from this study it can be concluded that the performance of resistive ZnO based sensors to NH_3 vapor can be controlled by tuning the morphology of the metal oxide thin film by a rapid synthesis procedure assisted by the spray pyrolysis method, providing a simple way to fabricate highly sensitive NH_3 vapor sensors.

REFERENCES

[1] Amritpal Singh, Praveen Kumar, Structural, morphological and optical properties of sol gel processed CdZnO nanostructured films:effect of precursor solvents, International Nano Letters (2013) 3:57.

[2] V.R. Shinde, T.P. Gujar, C.D. Lokhande, R.S. Mane, Sung-Hwan Han, Use of chemically synthesized ZnO thin film as a liquefied petroleum gas sensor, 137 (2007) 119–125.

[3] X.Y. Kong, Z.L. Wang, Spontaneous polarization-induced nanohelixes, nanosprings, and nanorings of piezoelectric nanobelts, Nano Letters 3 (2003) 1625–1631.

[4] K.S. Leschkies, R. Divakar, J. Basu, E.E. Pommer, J.E. Boercker, C.B. Carter, U.R.Kortshagen, D.J. Norris, E.S.Aydil, Photosensitization of ZnO nanowires with CdSe quantum dots for photovoltaic devices, Nano Lett. 7 (2007) 1793–1798.

[5] Y.N. Xia, P.D. Yang, Y.G. Sun, Y.Y.Wu, B. Mayers, B. Gates, Y.D. Yin, F. Kim, H.Q. Yan, One-dimensional nanostructures: synthesis, characterization, and applications, Adv. Mater. 15 (2003) 353–389.

[6] Hui Ping Wu, Lu Lin Li, Chien Chon Chen, Eric Wei Guang Diau, Anodic TiO2 Nanotube Arrays for Dye-Sensitized Solar Cells Characterized by Electrochemical Impedance Spectroscopy, Ceramics International 38 (2012) 6253–6266.

[7] Hee-Gon Bang, Jun-Ki Chung, Rae-Young Jung, Sang-Yeup Park, Effect of acetic acid in TiO2 paste on the performance of dye-sensitized solar cells, Ceramics International 38S (2012) S511–S515.

[8] S.Niranjan Ramgir, Manmeet Kaur, K. Preetam, Sharma, Niyanta Datta, S. Kailasaganapathi, S. Bhattacharya, A.K. Debnath, D.K. Aswal, S.K. Gupta, Ethanol sensing properties of pure and Au modified ZnO nanowires 187 (2013) 313-318.

[9] R. Pandeeswari, B.G. Jayaprakash, CeO2 thin fil as a low-temperature formaldehyde sensor in mixed vapour environment, Bull.Mater.Sci. 37 (2014) 1293-1299.

[10] S. Basu, A. Dutta, Modified heterojunction based on zinc oxide thin film for hydrogen gas-sensor application Sensors Actuators B 22 -1994. 83.

[11] Young-Sam Jin, Kyung-Hwan Kim, Woo-Jae Kim, Kyung-Uk Jang, Hyung-Wook Choi, The effect of RF-sputtered TiO2 passivating layer on the performance of dye sensitized solar cells, Ceramics International 38S (2012) S505–S509.

[12] O.Takai, M. Futsuhara, G.Shimizu, C.P. Lungu, J. Nozue, Nanostructure of ZnO thin films prepared by reactive RF magnetron sputtering. Thin Solid Films 1998, 318, 117-119.

[13] O.Goede and w.Hembrodt, 1988. An optical property of (Zn.Mn) chalcogenide mixes crystals and superlattices, Phys, Stat, Sol.B. 146:11-62.

[14] Y. Vijayakumar, Ganesh Kumar Mani, M.V.Ramana Reddy, John Bosco Balaguru Rayappan, Nanostructured flower likeV2O5 thin films and its room temperature sensing characteristics, Ceramics International 41(2015)2221–2227.

[15] Suk In Noh, Hyo-Jin Ahn, Doh-Hyung Riu, Photovoltaic property dependence of dye-sensitized solar cells on sheet resistance of FTO substrate deposited via spray pyrolysis, Ceramics International 38 (2012) 3735–3739.

[16] A.E. Jimenez-Gonzailez, P.K. Nair, Photosensitive ZnO thin films prepared by the chemical deposition method SlLAR, Semicond. Sci. Technol. 10 (1995) 1277–1281.

[17] N.L. Tarwala, A.V. Rajgured, A.I. Inamdara, R.S. Devane, I.Y. Kimf, S.S. Suryavanshid, Y.R. Mae, J.H. Kimf,, P.S. Patil , Growth of multifunctional ZnO thin films by spray pyrolysis technique, Sensors and Actuators A. 199 (2013) 67– 73.

[18] P. Mitra, A.P. Chatterjee, H.S. Maiti, ZnO thin film sensor, Materials Letters 35 1998 33–38.

[19] R. Ferro, The effect of the material morphology on the response of the NO2 sensor based on ZnO thin film, 143 (2009) 99–102.

[20] T.V. Vimalkumar, N. Poornima, C. Sudha Kartha, K.P. Vijayakumar, Effect of precursor medium on structural, electrical and optical properties of sprayed polycrystalline ZnO thin films, Materials Science and Engineering B. 175 (2010) 29–35.

[21] F. Paraguay and M. Miki-Yoshida, Doping effects on the response of thin film ZnO gas sensor to ethanol vapour, Superficies. 9 (1999) 245-247.

[22] Jiaqiang Xua, Jianjun Han, Yuan Zhang , Yu'an Sunc, Bing Xie , Studies on alcohol sensing mechanism of ZnO based gas sensors, Sensors and Actuators B: Chemical 132 (2008) 334–339.

[23] P.S. Shewale, G.L. Agawane, S.W. Shin, A.V. Moholkar, J.Y. Lee, J.H. Kim, M.D. Uplane, Thickness Dependent H2S Sensing Properties of Nanocrystalline ZnO Thin Films Derived by Advanced Spray Pyrolysis, Sensors and Actuators B: Chemical 177 (2013) 695–702.

[24] Nan Qin, Xiaohua Wang, Qun Xiang, Jiaqiang Xu, A biomimetic nest-like ZnO: Controllable synthesis and enhancedethanol response, Sensors and Actuators B: Chemical 191 (2014) 770– 778.

[25] Hugo Nguyen, Chu Thi Quy, Nguyen Duc Hoa, Nguyen The Lam, Nguyen Van Duy,Vu Van Quang, Nguyen Van Hieu, Controllable growth of ZnO nanowires grown on discrete islands of Au catalyst for realization of planar-type micro gas sensors, Sensors and Actuators B: Chemical 193 (2014) 888– 894.

[26] Shaohong Wei, Shaomei Wang, Yan Zhang, Meihua Zhou, Different morphologies of ZnO and their ethanol sensing property, Sensors and Actuators B : chemical 2 (2014) 480–487.

[27] P.B. Barna, M. Adamik, Fundamental structure forming phenomena of polycrystalline films and the structure zone models, Thin Solid Films 317 (1998) 27.-33.

[28] Min Su Kim, Kwang Gug Yim, Jeong-Sik Son, Jae-Young Leem, Effects of Al Concentration on Structural and Optical Properties of Al-doped ZnO Thin Films, Bull. Korean Chem. Soc. 2012, Vol. 33, No. 4 1235

[29] M. Saleem, L. Fang, H. B. Ruan, F. Wu1, Q. L. Huang, C. L. Xu and C. Y. Kong, Effect of zinc acetate concentration on the structural and optical properties of ZnO thin films deposited by Sol-Gel method, International Jl. Of Phyl Sci.7 (2012) 2971-2979.

[30] Jonnala Rakesh Reddy, Kovalakannan Sivalingam, Ganesh Kumar Mani, Prabakaran Shankar and John Bosco Balaguru Rayappan, Synthesis and Characterization of Sol-Gel Dip Coated Pure and Mn-Doped ZnO Thin Films, Research Jl. Of Pharamaceutical, Biological and Chemical Sci. (2014) 605-613.

[31] Nanda Shakti, P.S.Gupta, Structural and Optical Properties of Sol-gel Prepared ZnO Thin Film, Applied Physics Research Vol-2 (2010) 19-28.

[32] Said Benramache, Boubaker Benhaoua, Hamza Bentrah, Preparation of transparent, conductive ZnO:Co and ZnO:In thin films by ultrasonic spray method, Jl. Of Nanostructured in Chemistry. 3:54 (2013) 1-7.

[33] R.Ghosh, D.Basak, S.Fujihara, Effect of substrate-induced strain on the structural, optical and electrical properties of polycrystalline ZnO thin films, J. Appl. Phys. 96: (2004)2689-2692.

[34] M.F. Malek, M.H. Mama, Z. Khusaimi, M.Z. Sahdan, M.Z. Musa, A.R. Zainun, A.B. Suriani, N.D. Md Sin, S.B. Abd Hamid, M. Rusop, Sonicated sol–gel preparation of nanoparticulate ZnO thin films with various deposition speeds: The highly preferred c-axis (002) orientation enhances the final properties, Journal of Alloys and Compounds 582 (2014) 12–21.

[35] Sung-Soon Park, J.D. Mackenzie, Sol-gel-derived tin oxide thin films, Thin Solid Films 258 (1995) 268-273.

[36] J. Rodríguez-Báez, A. Maldonado, G. Torres-Delgado, R. Castanedo-Pérez, M. de la L. Olvera, Influence of the molar concentration and substrate temperature on fluorine-doped zinc oxide thin films chemically sprayed, Materials Letters 60 (2006) 1594–1598.

[37] P.S. Shewale, G.L. Agawane, S.W. Shin, A.V. Moholkar, J.Y. Lee, J.H. Kim, M.D. Uplane, Thickness Dependent H2S Sensing Properties of Nanocrystalline ZnO Thin Films Derived by Advanced Spray Pyrolysis, Sensors and Actuators B.(2012).

[38] Nguyen Le Hung, Hyojin Kim, Soon-Ku Hong, Dojin Kim, Enhancement of CO gas sensing properties in ZnO thin films deposited on self-assembled Au nanodots, Sensors and Actuators B: Chemical 151 (2010) 127–132.

[39] K.K. Makhija, Arabida Ray, R.M. Patel, U.B. Trivedi, H.N. Kapse, Indium oxide thin film based ammonia gas and ethanol vapour sensor, Bull. Mater. Sci. 28 (2005) 9-17.

[40] Yong-Liang, Tang Zhi-Jie Li, Jin-Yi Ma, Yuan-Jun Guo, Yong-Qing Fu, Xiao-Tao Zu, Ammonia gas sensors based on ZnO/SiO2 bi-layer nanofilms on ST-cut quartz surface acoustic wave devices (2014).

APPENDIX

Table – 1: *Variation of Texture Co-efficient with Concentration*

S.No	Solution concentration	TC(101)	TC(100)	TC(002)	TC(110)
1	0.05M	1.12	1.00	0.87	-
2	0.1M	1.70	1.20	0.73	0.34
3	0.15M	1.71	1.12	0.67	0.50
4	0.2M	1.58	1.27	0.74	0.41

Table – 2: *Variation of Strain, Strain%, Dislocation, Specific Surface Area and Optical Band Gap as a Function of Concentration*

S.No	Solution concentration	Micro strain 10^{-3}	Strain%	δ 10^{3} $(nm)^{-2}$	Specific surface area (A) M^2/kg	Crystallite size D (nm)	Optical band gap (eV)
1	0.05M	0.4	0.293	0.1608	1.35	7.8	3.25
2	0.1M	2.0	-4.63	4.0389	8.98	10.8	3.27
3	0.15M	2.7	-4.57	7.0403	6.80	11.5	3.37
4	0.2M	2.4	-4.51	5.8183	8.16	15.7	3.32

Table – 3: *Variation of Lattice Parameters as a Function of Concentration*

S.No	Solution concentration	a(Å)	c(Å)	c/a
1	**0.05M**	**3.013**	**5.22033**	**1.732**
2	**0.1M**	**2.866**	**4.964**	**1.732**
3	**0.15M**	**2.867**	**4.967**	**1.732**
4	**0.2M**	**2.869**	**4.970**	**1.732**

Table – 4: *Variation of Sensing Parameters as a Function of Ammonia Vapor Concentration*

Ammonia vapor concentration(ppm)	Response time (sec)	Recovery time (sec)	Sensing response (%)
10	90	37	94
20	86	39	183

30	79	67	351
40	71	85	520
50	69	103	833

Figure-1: *Illustration of the Formation Mechanism of Spray Deposited ZnO Thin Film*

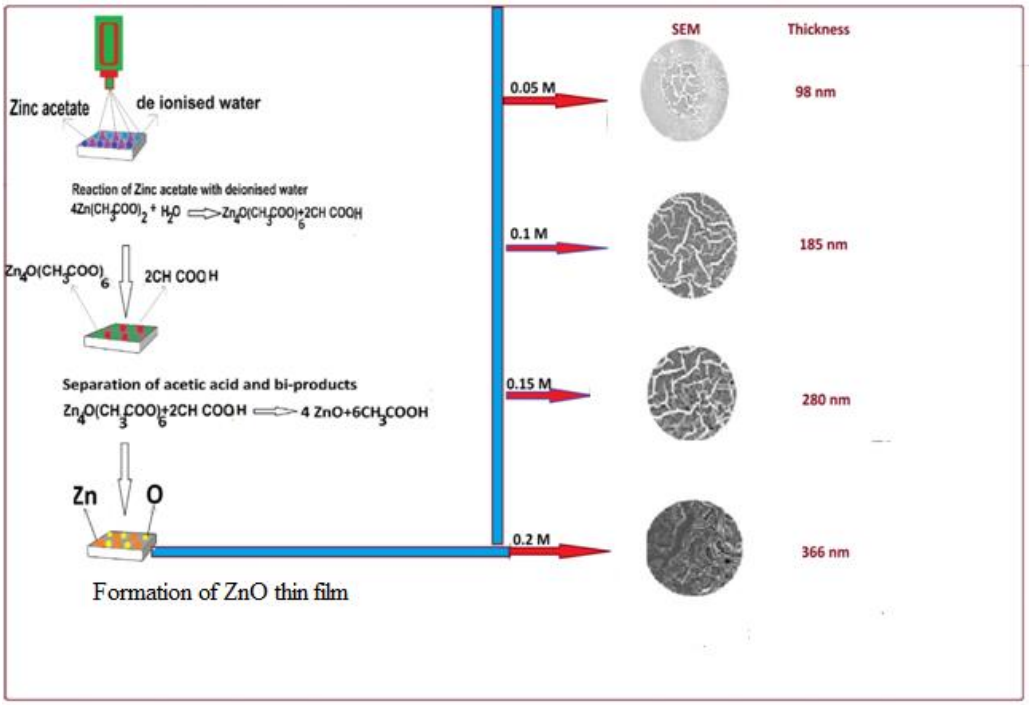

Figure-2: *XRD Pattern of ZnO Thin Films Obtained from Different Precursor Solution Concentrations*

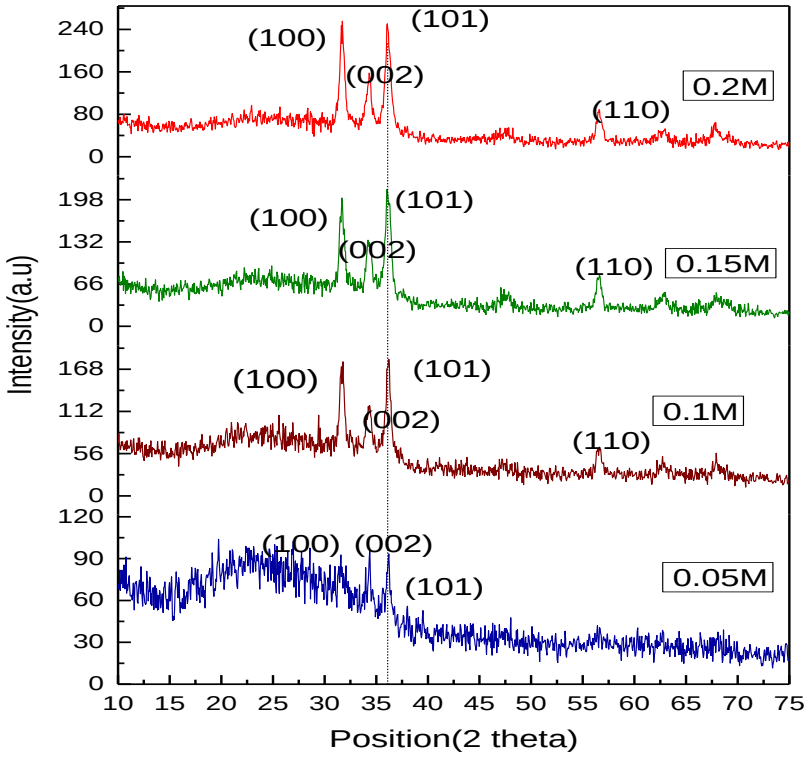

Figure-3: *FESEM Images of ZnO Films Deposited at Various Concentrations in the Range of 1µm*

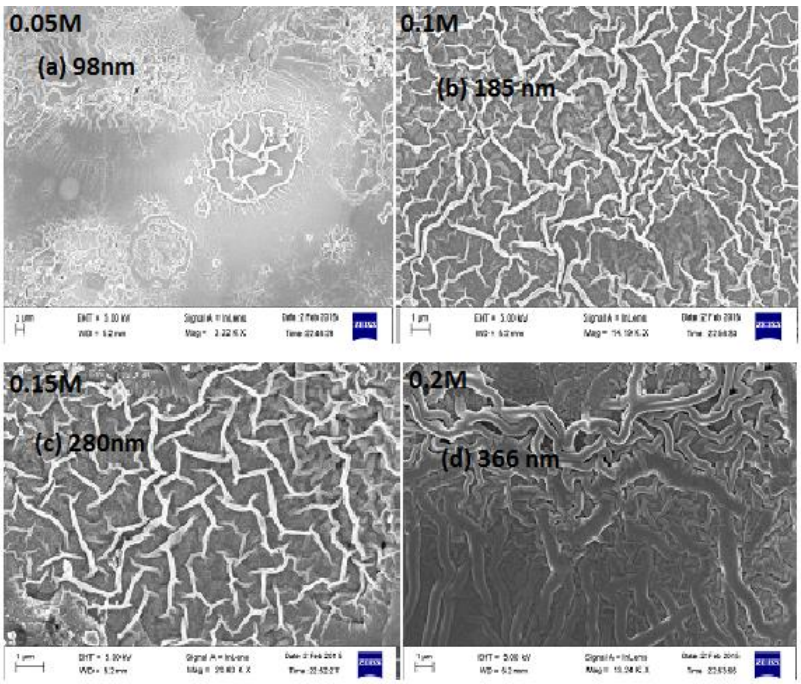

Figure-4: *Surface Topography Variation of the ZnO Thin Film (a) 2D Image and (b) 3D Image 0.1M Over a Scale of 2µm× 2µm*

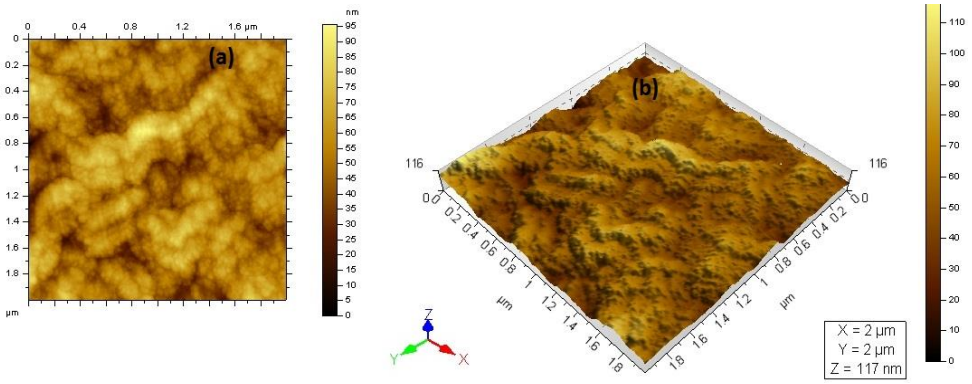

Figure-5: *Surface Topography Variation of the ZnO Thin Film (a) 2D Image and (b) 3D Image 0.2M Over a Scale of 5µm× 5µm*

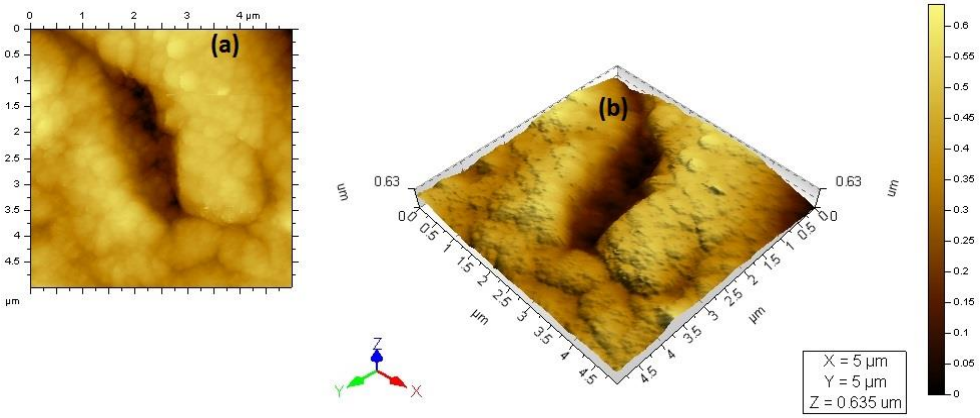

Figure-6: *Optical Absorbance Spectra of ZnO Thin Films Deposited at Various Concentrations as a Function of Wavelength*

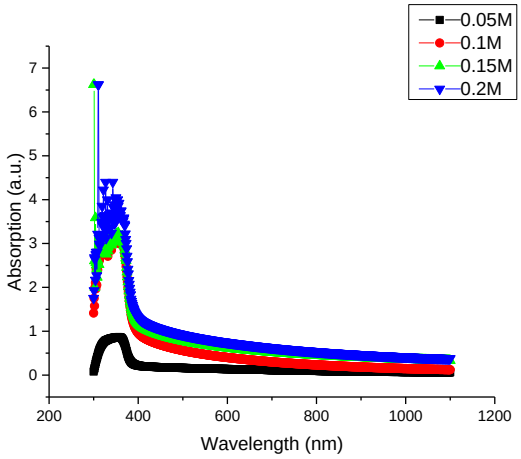

Figure-7: *Optical Transmission Spectra of ZnO Thin Films Deposited at Various Concentrations as a Function of Wavelength*

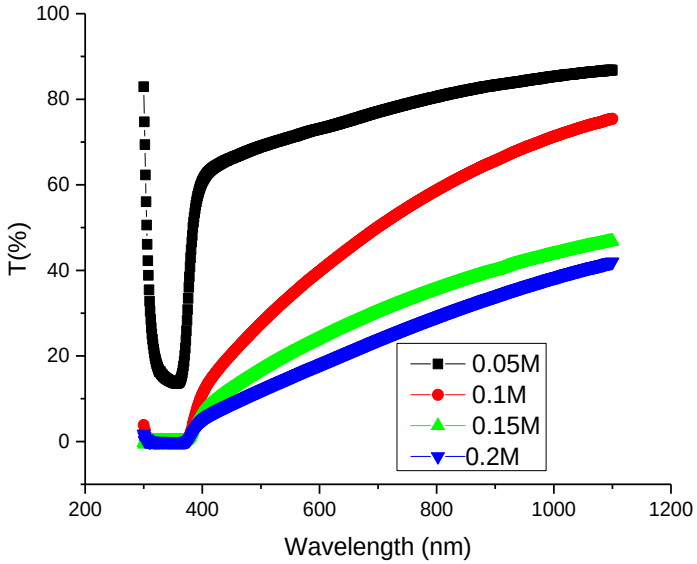

Figure-8: *Estimates of the Optical Band Gap Energy (Eg) of ZnO Thin Films Using Tauc's Plot as a Function of Concentration*

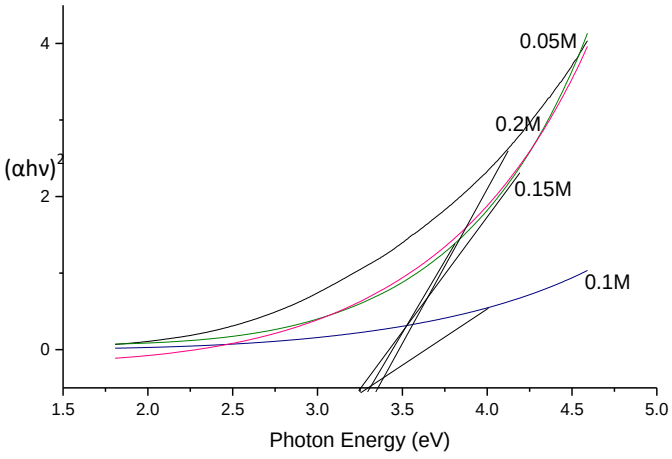

Figure-9: *Various Vapor Sensing Response (%) of 0.1M ZnO Film at 300oC Operating Temperature for 50 ppm Vapor Concentration*

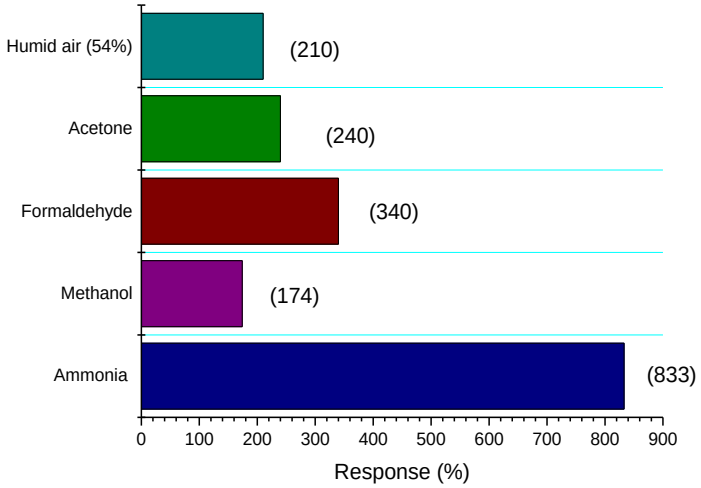

Figure-10: *Vapor Selectivity of 0.1M ZnO Film at 300oC*

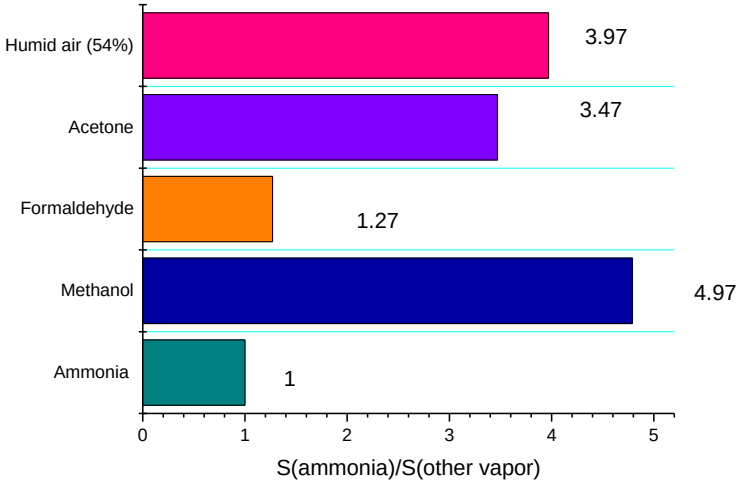

Figure-11: *Temperature Dependence of the Sensing Response (%) of 50 ppm Ammonia Vapor Concentration for the ZnO Thin Film*

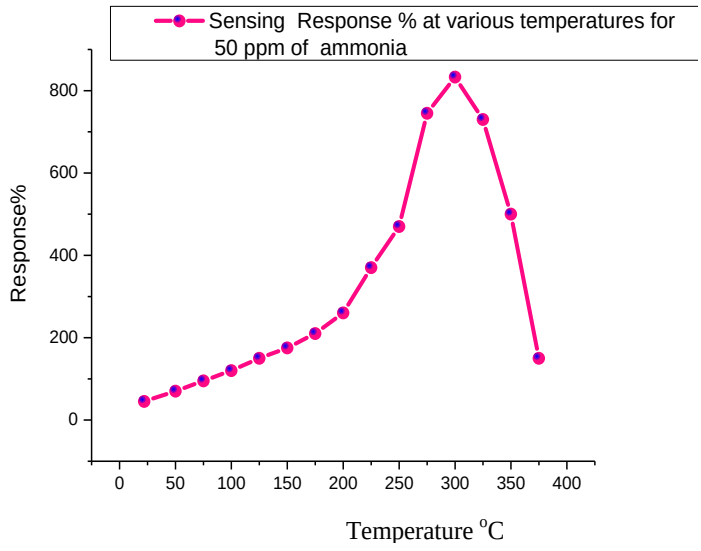

Figure-12: *Schematic Diagram of the Possible Ammonia Sensing Process of ZnO Sensor*

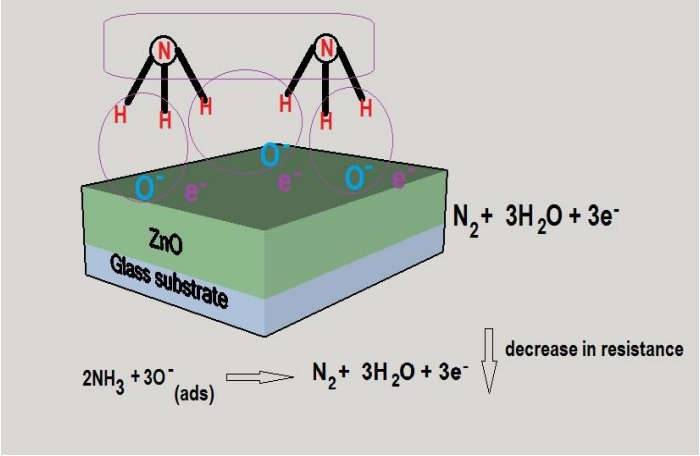

Figure-13: *Transient Resistance Response of ZnO Sensor to Exposure of Various Concentrations of NH3 at 300oC Figure*

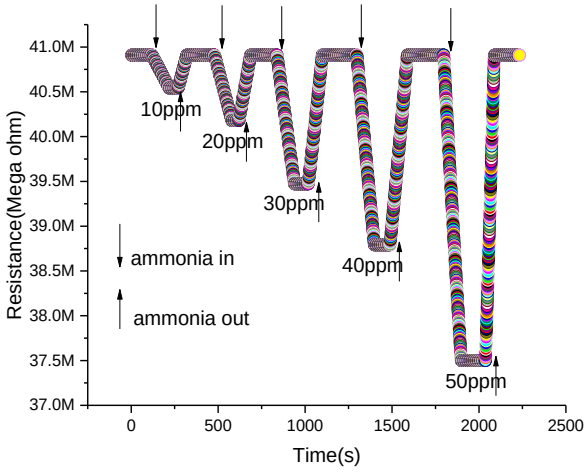

Figure-14: *Transient Resistance Response of ZnO Sensor to Exposure of 10ppm of NH3 at 300oC*

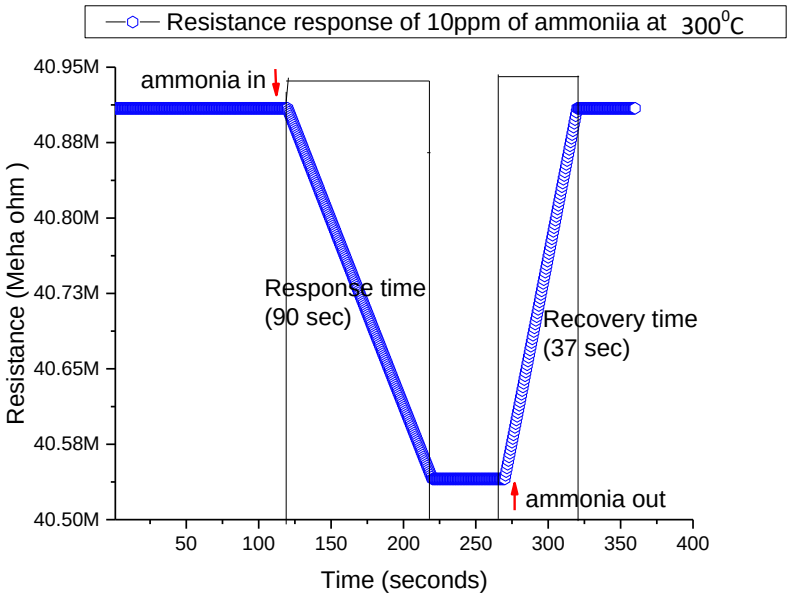

Figure-15: *Sensitivity of the ZnO Sensor at 300oC at Various Concentrations of Ammonia*